

- Rottman, *Genes Dev.* **7**, 2598 (1993).
10. M. Ayane, U. Preuss, G. Köhler, P. J. Nielsen, *Nucleic Acids Res.* **19**, 1273 (1991); M. Vellard, A. Sureau, J. Soret, C. Martinierie, B. Perbal, *Proc. Natl. Acad. Sci. U.S.A.* **89**, 2511 (1992); X.-D. Fu and T. Maniatis, *Science* **256**, 535 (1992).
 11. A. Hanamura and A. R. Krainer, unpublished results.
 12. A. R. Krainer, T. Maniatis, B. Ruskin, M. R. Green, *Cell* **36**, 993 (1984).
 13. R. Treisman, S. H. Orkin, T. Maniatis, *Nature* **302**, 591 (1983).
 14. For transfection of HeLa cells, 5 μ g of the β^{thal} plasmid and 0.5 or 1 μ g of pCG-SF2 (or pCG) were added to a 60-mm dish of 60 to 75% confluent HeLa cells in the presence of 20 μ g of lipofectin (Gibco-BRL). Cells were harvested 48 hours after transfection and lysed with NP-40, and total RNA was purified as described [M. Z. Gilman, *Current Protocols in Molecular Biology*, F. M. Ausubel et al., Eds. (Wiley, New York, 1988, vol. 1, pp. 4.1.2–4.1.3)]. Total RNA (200 ng) was analyzed by RT-PCR with thermostable DNA polymerase from *Thermus thermophilus* (Epicentre, Madison, WI). Aliquots of each RNA sample were analyzed with the appropriate set of β -globin or SF2/ASF primers. The oligonucleotides used for β -globin detection were TCAAACGACACCATGTGACACCTGACT, as an exon 1 forward primer, and CAGGAGTGGACAGATCCC, as an exon 2 reverse primer. The oligos used for SF2/ASF detection were GACGCCATCCACGCTGTT, which is specific for the 5' untranslated region (UTR) derived from the pCG vector (24), and TCGAGTCCGCGCTTTTCG, which is specific for the 5' UTR of the endogenous SF2/ASF gene; both of these were used as forward primers, and GCTTCGAGGAACTCCAC was used as a reverse primer. All three SF2/ASF primers were present in the same reaction. In these and the following RT-PCR reactions, the different RNA species were amplified simultaneously with at least one common primer. In addition, the number of cycles was minimized to maintain linearity, and the relative abundance of the SF2/ASF mRNAs was verified by primer extension (21).
 15. HeLa cells were separately transfected with a plasmid expressing the *Escherichia coli lacZ* gene [R. R. Spaete and E. S. Mocarski, *J. Virol.* **56**, 135 (1985)], followed by staining with X-gal to measure the transfection efficiency. Approximately 5% of the cells expressed the transfected DNA (21). Because similar amounts of SF2/ASF mRNA transcribed from endogenous and transfected genes were measured in the total cell population (Fig. 1B), we conclude that the overall expression of SF2/ASF mRNA in the transfected cells increased approximately 20-fold, on average. The relative efficiencies with which the endogenous and exogenous SF2/ASF mRNAs are translated are not known, because the proteins are indistinguishable.
 16. S. Stamm et al., *Nucleic Acids Res.* **20**, 5097 (1992).
 17. W. Guo, G. J. Mulligan, S. Wormsley, D. M. Helfman, *Genes Dev.* **5**, 2096 (1991).
 18. D. M. Helfman, W. M. Ricci, L. A. Finn, *ibid.* **2**, 1627 (1988).
 19. W. Guo and D. M. Helfman, *Nucleic Acids Res.* **21**, 4762 (1993).
 20. We transfected 5 μ g of the tropomyosin minigene plasmid pSV40-p2 (18) into HeLa cells with or without SF2/ASF or control plasmids, as described (14). Aliquots of each RNA sample were analyzed by RT-PCR with a 5' end-labeled forward primer homologous to the SV40 5' UTR and a reverse primer complementary to either exon 9 (Fig. 3A) or to exon 6 (Fig. 3B), as described (19). A reverse primer complementary to exon 5 was also present in the RT-PCR reactions; the resulting amplification product serves to normalize with respect to all tropomyosin minigene transcripts (19). The RT-PCR products were quantitated on a Fujix BAS2000 PhosphorImager.
 21. J. F. Cáceres and A. R. Krainer, unpublished results.
 22. C. Svensson, U. Pettersson, G. Akusjärvi, *J. Mol. Biol.* **165**, 475 (1983).
 23. More efficient expression of transfected hnRNP A1 and a corresponding change in E1A alternative splicing can be achieved with the use of a mouse erythroleukemia cell line that expresses only trace amounts of endogenous hnRNP A1 [X. Yang et al., *Proc. Natl. Acad. Sci. U.S.A.* **91**, 6924 (1994)].
 24. M. Tanaka and W. Herr, *Cell* **60**, 375 (1990).
 25. The β -globin expression vector (pUC β 128SV) consists of a Hind III–Pst I fragment of wild-type human β -globin from π SVHP β 128 [R. Treisman, M. R. Green, T. Maniatis, *Proc. Natl. Acad. Sci. U.S.A.* **80**, 7428 (1983)] subcloned into the corresponding sites of pUC19 and an SV40 Pvu II–Nco I enhancer fragment from the same plasmid subcloned into the Sma I–Hinc II sites. The β -thalassemia expression plasmid was constructed by the replacement of an Nco I–Bam HI β -globin fragment of pUC β 128SV with the corresponding fragment of the β^{thal} allele from SP64-H β Δ 6IVS1-1A (12). The SF2/ASF expression plasmid pCG-SF2 was constructed by subcloning an Nde I (blunted)–Bam HI fragment of pET9c-SF2 (3) into pCG (24) cleaved with Xba I and Bam HI. The Xba I end was first treated with T4 DNA polymerase in the presence of deoxyadenosine triphosphate, followed by digestion with mung bean nuclease. The resulting plasmid contains the full-length natural SF2/ASF coding sequence.
 26. J. P. Morgenstern and H. Land, *Nucleic Acids Res.* **18**, 1068 (1990).
 27. Detection of the unspliced pre-mRNA with the SV40 and exon 6 primers (Fig. 3B) but not with the SV40 and exon 9 primers (Fig. 3A) is probably due to inefficient amplification of the much longer product with the latter set of primers. Likewise, increased 5, 6 splicing upon SF2/ASF overexpression is more evident with the exon 6 primer (Fig. 3B), probably because RNA molecules that still retain one or more of the remaining introns amplify inefficiently with the exon 9 primer (Fig. 3A). We note that the amounts of unspliced pre-mRNA seldom remain unchanged when the selection of alternative splice sites is modulated by SF2/ASF or hnRNP A1, and this is also the case in vitro (1, 5). This is probably because the overall splicing efficiency differs according to which splice sites have been selected.
 28. A. J. Berk and P. A. Sharp, *Cell* **14**, 695 (1978); M. Perriacaudet, G. Akusjärvi, A. Virtanen, U. Pettersson, *Nature* **281**, 694 (1979).
 29. C. Stephens and E. Harlow, *EMBO J.* **6**, 2027 (1987).
 30. B. Zerler et al., *Mol. Cell. Biol.* **6**, 887 (1986).
 31. We thank M. Tanaka for the pCG vector, B. Moran for the pMTE1A vector, V. Chua for constructing pCG-A1, and W. Guo for reagents and advice about β -tropomyosin assays. We are grateful to M. Tanaka and A. Stenlund for helpful discussions and to B. Stillman and A. Mayeda for critical reading of the manuscript. S.S. was supported by the Deutsche Forschungsgemeinschaft. D.M.H. is an Established Investigator of the American Heart Association. A.R.K. is a Pew Scholar in the Biomedical Sciences. Supported by grants from the National Cancer Institute (A.R.K.) and NIH (D.M.H.).

14 June 1994; accepted 11 August 1994

Coaxially Stacked RNA Helices in the Catalytic Center of the *Tetrahymena* Ribozyme

Felicia L. Murphy, Yuh-Hwa Wang, Jack D. Griffith, Thomas R. Cech*

Coaxial stacking of helical elements is a determinant of three-dimensional structure in RNA. In the catalytic center of the *Tetrahymena* group I intron, helices P4 and P6 are part of a tertiary structural domain that folds independently of the remainder of the intron. When P4 and P6 were fused with a phosphodiester linkage, the resulting RNA retained the detailed tertiary interactions characteristic of the native P4-P6 domain and even required lower magnesium ion concentrations for folding. These results indicate that P4 and P6 are coaxial in the P4-P6 domain and, therefore, in the native ribozyme. Helix fusion could provide a general method for identifying pairs of coaxially stacked helices in biological RNA molecules.

Many RNA molecules require specific three-dimensional structures for their biological activity. Determination of RNA secondary structure (base-paired helices, bulges, and hairpin loops) is now relatively straightforward (1). Bridging the gap from a secondary structure to a three-dimensional structure, on the other hand, remains problematic. The only biologically active RNAs whose structures have been resolved at the atomic level by x-ray crystallography are transfer RNAs (tRNAs) (2).

RNA secondary structures often have three or more helical elements diverging

from a central wheel, as in the tRNA cloverleaf. Other examples are found in ribosomal RNAs (rRNAs) (3), group I and group II self-splicing introns (4, 5), small nuclear RNAs (6), and the human immunodeficiency virus (HIV) Rev response element (7). In tRNA, pairs of adjacent RNA helices share the same helix axis; this is the case for the aminoacyl acceptor and T stems and also for the anticodon and D stems. Such arrangements are expected to be favorable because of the energetic contribution of base stacking. If coaxially stacked helices could be identified in an unknown RNA structure, then the overall architecture of the molecule would begin to become apparent, and a constraint for modeling would be provided.

Catalytic RNAs (ribozymes) provide systems for addressing questions of RNA structure because their structural integrity is re-

F. L. Murphy and T. R. Cech, Howard Hughes Medical Institute, Department of Chemistry and Biochemistry, University of Colorado, Boulder, CO 80309, USA.
Y.-H. Wang and J. D. Griffith, Lineberger Comprehensive Cancer Center, University of North Carolina, Chapel Hill, NC 27599, USA.

*To whom correspondence should be addressed.

flected in the reactions they catalyze (8). The catalytic center common to group I introns contains four closely linked helices,

paired regions P3, P4, P6, and P7 (Fig. 1A). Two of these, P4 and P6, are in the same structural domain—a portion of the intron

capable of folding into its correct secondary and tertiary structure in the absence of the remainder of the intron (9, 10). In the

Fig. 1. Secondary structure of the P4-P6 domain of the *Tetrahymena* ribozyme and design of the P4-P6 fusion RNA. **(A)** Structural model of the *Tetrahymena* self-splicing intron (4) displayed in the format of Burke and co-workers (33). Solid arrows indicate 5' and 3' splice sites. Nucleotide sequence shown in paired regions P3, P4, P6, and P7 and adjacent single-stranded nucleotides highlights the catalytic center of the ribozyme. Heavy dashed line indicates the phosphodiester linkage we introduced to create the P4-P6 fusion RNA; its 5' and 3' termini are also indicated. Nucleotide numbers refer to the excised intron. **(B)** The P4-P6 domain represented according to Cech and co-workers (34). P4 is coaxially stacked on P6. Boxed nucleotides connected by solid lines indicate the long-range tertiary interaction between the GAAA loop and P6a (10) and the triple-strand regions involving P4 and P6 (12, 13, 29). We introduced the dashed lines indicating the covalent phosphodiester backbone to avoid a crowded representation; the lines do not represent additional nucleotides. In the mutant called J5/5a paired, we mutated the nucleotides involved in the bend at the top of the diagram to give a continuous base-paired helix between P5 and P5a, thereby destabilizing the bend (9).

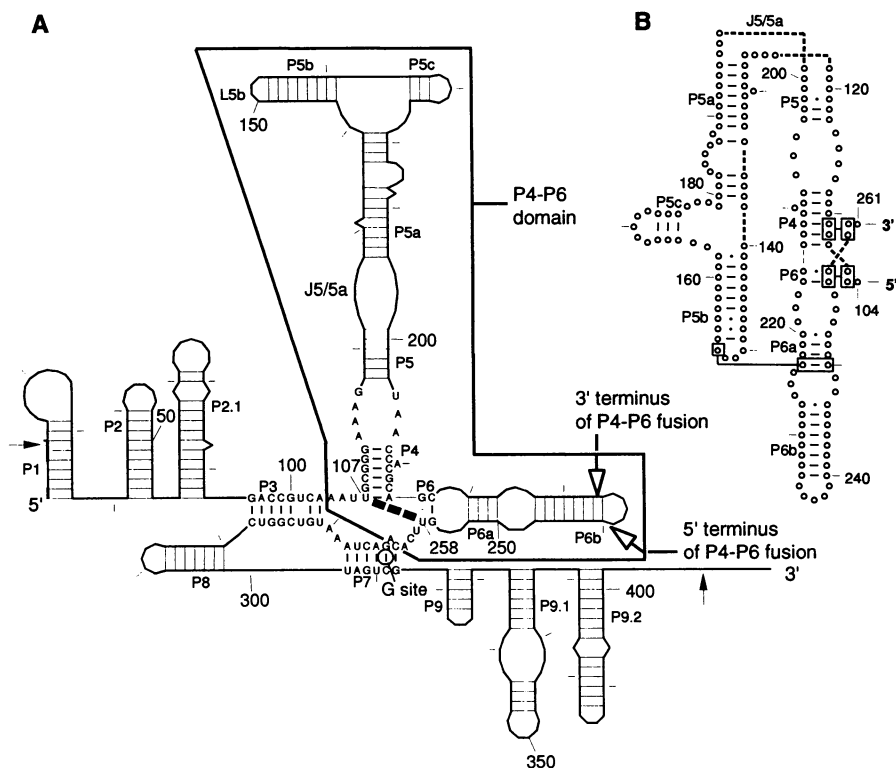
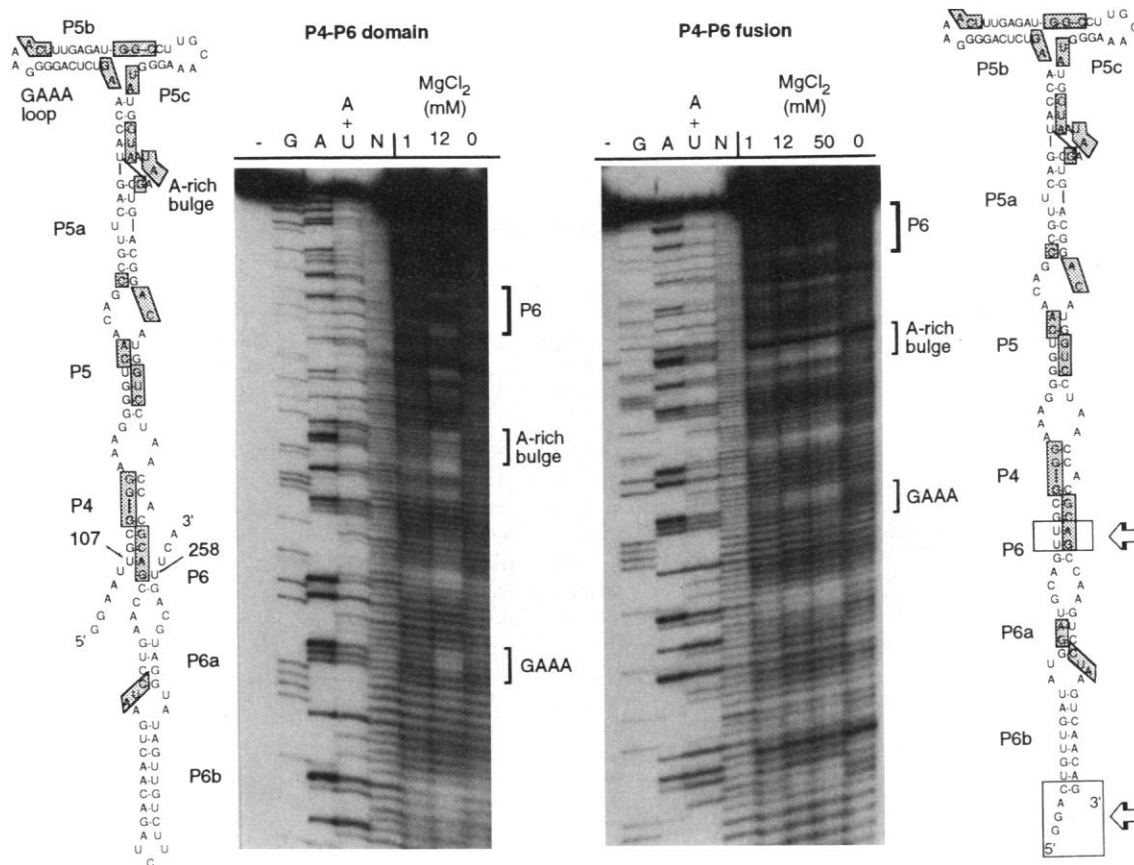


Fig. 2. The P4-P6 fusion RNA shows the detailed Fe(II)-EDTA cleavage-protection pattern characteristic of the native domain (35). The minus sign indicates a lane of untreated RNA. Sequence ladders for guanosine (G), adenosine (A), adenosine plus uridine (A + U), or any nucleotide (N) produced by limited treatment with ribonucleases or alkali (36). RNA cleaved by Fe(II)-EDTA in the presence of the indicated $MgCl_2$ concentrations is shown; a decrease in intensity of an area of a lane after addition of $MgCl_2$ represents protection from cleavage by RNA folding. Structural diagrams of the native and fusion domains at left and at right, respectively, are extended versions of that shown in Fig. 1B; sites of protection from Fe(II)-EDTA cleavage are boxed and shaded. The 5'-GA-3' in P6a, which was protected in the P4-P6 fusion molecule, was too close to the 3' end of the native P4-P6 domain for us to confirm its protection. Sites of altered connectivity in P4-P6 fusion are boxed and denoted by arrows.



standard secondary structure diagram of group I introns, P4 and P6 are represented as being perpendicular. However, the 3' nucleotide of P4 (A214) is immediately adjacent to the 5' nucleotide of P6 (G215), and researchers have modeled these two duplexes as sharing the same helix axis (11–13) (Fig. 1B).

To provide a test of the coaxial stacking of P4 and P6, we constructed a circularly permuted version (14) of the P4-P6 tertiary structure domain in which U258 at the 3' end of P6 was directly linked to U107 at the 5' end of P4 (Fig. 1A). In this P4-P6 fusion construct, the ends of the RNA are in the region usually capped off by the P6b hairpin loop, a loop which is not itself important for intron function (15) or for higher-order structure of the P4-P6 domain (9, 10). If the three-dimensional structure of the domain involved juxtaposition of the P4 and P6 helices at an angle, then we

could expect the fusion of these elements to disrupt or destabilize the native tertiary structure. On the other hand, if P4 and P6 were coaxially stacked in the native molecule, then their fusion might be structurally inconsequential.

We compared the tertiary structures of the native P4-P6 domain and the circularly permuted P4-P6 fusion molecule using solvent-based Fe(II)-EDTA as a structural probe (16). Higher order folding of the P4-P6 domain in the presence of 12 mM Mg^{2+} gave a discrete pattern of protection from Fe(II)-EDTA cleavage (Fig. 2, left), the same pattern that had already been established (9). Each blank region in the cleavage pattern can be thought of as a footprint, a portion of the RNA that is protected by interaction with another portion of the same molecule. The P4-P6 fusion RNA gave the same pattern, but in this case protection had largely been established in 1 mM $MgCl_2$ (Fig. 2, right).

The Fe(II)-EDTA protection pattern is an indicator of structural integrity. Other work has shown that protected regions become accessible after disruption of the RNA tertiary structure by mutations in internal loop J5/5a that force the loop to become base-paired (the J5/5a paired mutant) (9) or by single-base mutations in the GAAA tetraloop of P5b or in the A-rich bulge of P5a (10). Thus, the maintenance of the same detailed pattern of protection in the P4-P6 fusion RNA provides evidence that it folds into a three-dimensional structure similar to that of the native domain. The Mg^{2+} requirement reflects the stability of the intron (17) or of the isolated domain (9, 10). Increasing the Mg^{2+} concentration causes structural defects in mutant introns to be suppressed (18). The reduced Mg^{2+} requirement for folding of the P4-P6 fusion

RNA therefore suggests that fixing P4 and P6 in a helical geometry actually stabilizes the correct higher order structure of the entire domain (19).

Direct visualization of the P4-P6 fusion RNA by electron microscopy in the presence of Mg^{2+} (20) revealed that it had a compact structure indistinguishable from that of the native P4-P6 domain (Fig. 3, A and B). The frequency of compact forms relative to the total population was similar for the native domain and the P4-P6 fusion RNA (93 and 97%, respectively). These compact molecules had a diameter consistent with an RNA duplex folded on itself (21). In contrast, mutations such as J5/5a paired, which disrupt the long-range tertiary structure of the domain (9, 10), caused the RNA to appear rodlike (83% of the total molecules), with a length of 17.8 ± 1.6 nm, as expected for the molecule if it had only secondary structure [66 ± 6 base pairs (bp)] but no long-range tertiary structure (Fig. 3C) (21). In the absence of Mg^{2+} , with spermidine as the only multivalent counterion (20), the frequency of the compact molecules of the native domain was reduced (9% of the total). This is expected because of the known Mg^{2+} dependence of tertiary structure formation of the native domain. Under the same conditions, the P4-P6 fusion RNA showed 63% compact forms, implying greater stability of the P4-P6 fusion molecule.

Nondenaturing gel electrophoresis provided another test of the structural integrity of the RNA domain. Although bent DNA and RNA double helical molecules generally have retarded electrophoretic mobilities (22), the folded P4-P6 RNA domain runs faster than a duplex with the same number of base pairs; presumably, it is not just bent but also compact and in a size range where mean end-to-end distance dictates mobility (23). A number of mutations that disrupt the domain tertiary structure cause the RNA to migrate with a reduced mobility (23) that we infer to be characteristic of an extended helical form (24). When we applied this test to the P4-P6 fusion RNA, the RNA was found to comigrate with the native RNA domain with a mobility characteristic of a compact, rather than an extended, conformation (Fig. 4).

In summary, a molecule in which P4 and P6 are forced together by covalent linkage still forms the correct three-dimensional structure, as judged by Fe(II)-EDTA cleavage, electron microscopy, and nondenaturing gel electrophoresis. We therefore conclude that paired regions P4 and P6 are coaxially stacked in the native domain. Because the structure of the isolated P4-P6 domain is the same as its structure in the intact intron (9), we infer that P4 and P6 are coaxial in the active ribozyme. A test for coaxial stacking similar to ours has been

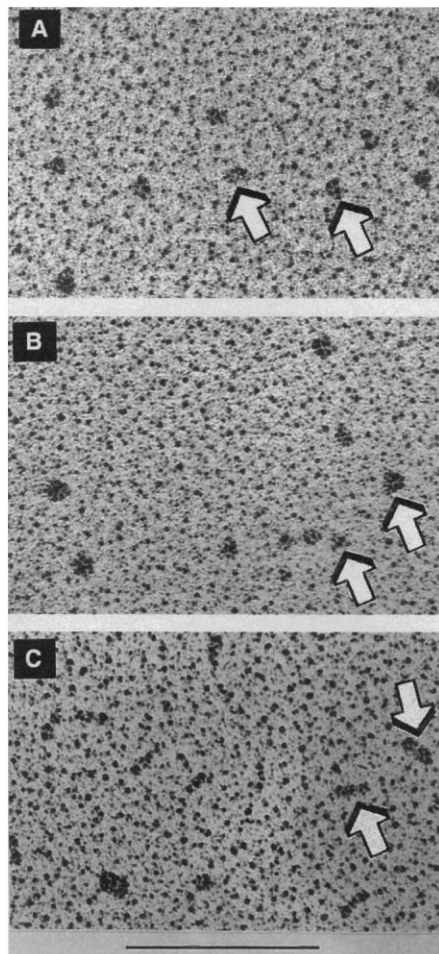


Fig. 3. Electron microscopic visualization of native and variant forms of P4-P6 RNA (20). (A) The P4-P6 fusion RNA and (B) the native P4-P6 domain exhibit compact structures. (C) The J5/5a paired mutant has a disrupted tertiary structure and appears in an extended rod-like form characteristic of its secondary structure. Arrows point to representative molecules. Bar is 100 nm.

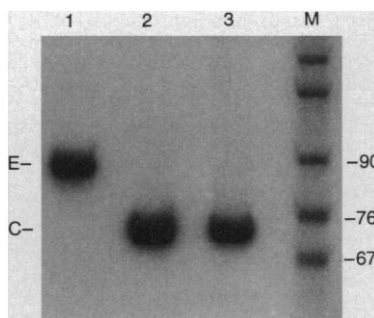


Fig. 4. P4-P6 RNA has a compact structure (C) by nondenaturing gel electrophoresis (37). Lane 1, J5/5a paired mutant RNA with an extended (E) structure. Lane 2, P4-P6 fusion RNA. Lane 3, native P4-P6 domain RNA. Lane M, marker double-stranded DNA fragments produced by *Msp*I digestion of pBR322; sizes in base pairs are indicated at the right. Upper region of gel (23) contained additional species, presumably intermolecular, that were low in abundance and variable between experiments.

performed for two stems in the hairpin ribozyme, with the opposite result: A joining segment of five or more nucleotides was required for efficient ribozyme action, and reduction to a single nucleotide bulge was inhibitory (25). It was therefore concluded that the helices are positioned at an angle, rather than coaxially, in the active structure (25). Helix fusion should provide a general test for the coaxial stacking of RNA stems. The positive result—the fusion is nondisruptive—indicates coaxial stacking, whereas the negative result would not rule out coaxial stacking, because it is conceivable that covalent linkage might alter helix phasing or prevent some flexibility required for the RNA structure and function.

What is the functional importance of coaxially stacked P4 and P6? The P4 and P6 duplexes and the adjacent P4-P5 internal loop contain some of the sequences that are the most highly conserved among diverse group I introns (13, 26). The P4-P5 loop, which researchers have proposed organizes the guanosine-binding site in P7 relative to the reaction site in P1 (27), is positioned in the active site by P4, always a 6-bp helix (26). Researchers have proposed that the strand leading into P4 and the strand exiting P6 form a triple helical scaffold (Fig. 1B), on the basis of phylogenetic analysis and site-specific mutagenesis (12), in vitro selection experiments (28), and nuclear magnetic resonance spectroscopy of model P4-P6 systems (29). The triple helical scaffold may stabilize the coaxially stacked P4 and P6 helices, help orient the rest of the catalytic core relative to the P4-P6 domain, or both.

It remains to be tested whether the P4-P6 fusion RNA could assemble with other portions of the intron to reconstitute an active ribozyme of altered connectivity. Such a multicomponent group I intron might even exist in nature.

REFERENCES AND NOTES

1. Successful methods for secondary structure determination include comparative sequence analysis of homologous RNAs from nature [C. R. Woese and N. R. Pace, in *The RNA World*, R. F. Gesteland and J. F. Atkins, Eds. (Cold Spring Harbor Laboratory Press, Cold Spring Harbor, NY, 1993), pp. 91–117] or of RNAs selected in vitro [L. Gold *et al.*, in *ibid.*, pp. 497–509] and mutagenesis, followed by analysis of second-site suppressors that restore activity by restoring base-pairing [T. R. Cech, *Annu. Rev. Biochem.* **59**, 543 (1990)].
2. S.-H. Kim *et al.*, *Science* **179**, 285 (1973); J. D. Robertus *et al.*, *Nature* **250**, 546 (1974).
3. H. F. Noller and C. R. Woese, *Science* **212**, 403 (1981).
4. F. Michel and B. Dujon, *EMBO J.* **2**, 33 (1983); R. B. Waring, C. Scazzocchio, T. A. Brown, R. W. Davies, *J. Mol. Biol.* **167**, 595 (1983).
5. F. Michel, K. Umeson, H. Ozeki, *Gene* **82**, 5 (1989).
6. S. J. Baserga and J. A. Steitz, in *The RNA World*, R. F. Gesteland and J. F. Atkins, Eds. (Cold Spring Harbor Laboratory Press, Cold Spring Harbor, NY, 1993), pp. 359–381.
7. E. T. Dayton, D. M. Powell, A. I. Dayton, *Science* **246**, 1625 (1989); M. H. Malim *et al.*, *Cell* **60**, 675 (1990); H. S. Olsen, P. Nelbock, A. W. Cochrane, C. A. Rosen, *Science* **247**, 845 (1990).
8. T. R. Cech, in *The RNA World*, R. F. Gesteland and J. F. Atkins, Eds. (Cold Spring Harbor Laboratory Press, Cold Spring Harbor, NY, 1993), pp. 239–269.
9. F. L. Murphy and T. R. Cech, *Biochemistry* **32**, 5291 (1993).
10. ———, *J. Mol. Biol.* **236**, 49 (1994).
11. S.-H. Kim and T. R. Cech, *Proc. Natl. Acad. Sci. U.S.A.* **84**, 8788 (1987).
12. F. Michel, A. D. Ellington, S. Couture, J. W. Szostak, *Nature* **347**, 578 (1990).
13. F. Michel and E. Westhof, *J. Mol. Biol.* **216**, 585 (1990).
14. T. Pan, R. R. Gutell, O. C. Uhlenbeck, *Science* **254**, 1361 (1991); M. Puttaraju and M. D. Been, *Nucleic Acids Res.* **20**, 5257 (1992); K. A. Jarrell, *Proc. Natl. Acad. Sci. U.S.A.* **90**, 8624 (1993); J. M. Nolan, D. H. Burke, N. R. Pace, *Science* **261**, 762 (1993).
15. J. V. Price, G. L. Kieft, J. R. Kent, E. L. Sievers, T. R. Cech, *Nucleic Acids Res.* **13**, 1871 (1985); G. F. Joyce, G. van der Horst, T. Inoue, *ibid.* **17**, 7879 (1989).
16. This reagent cleaves the nucleic acid backbone in a free radical reaction [R. Hertzberg and P. B. Dervan, *Biochemistry* **23**, 3934 (1984); T. D. Tullius and B. A. Dombroski, *Science* **230**, 679 (1985); *Proc. Natl. Acad. Sci. U.S.A.* **83**, 5469 (1986)]. The reaction is insensitive to secondary structure, with single- and double-stranded RNA cleaved with similar efficiency [D. W. Celander and T. R. Cech, *Biochemistry* **29**, 1355 (1990)]. However, it provides a test of tertiary structure because reactivity depends on the surface accessibility of each ribose [J. A. Latham and T. R. Cech, *Science* **245**, 276 (1989)].
17. D. W. Celander and T. R. Cech, *Science* **251**, 401 (1991).
18. J. M. Burke *et al.*, *Cell* **45**, 167 (1986); P. Flor, J. B. Flanagan, T. R. Cech, *EMBO J.* **8**, 3391 (1989); A. A. Beaudry and G. F. Joyce, *Biochemistry* **29**, 6534 (1990); F. Michel *et al.*, *Genes Dev.* **6**, 1373 (1992); A. J. Zaugg, M. J. McEvoy, T. R. Cech, *Biochemistry* **32**, 7946 (1993); B. Lagerbauer, F. L. Murphy, T. R. Cech, *EMBO J.* **13**, 2669 (1994).
19. The P4-P6 fusion RNA lacks the 5' and 3' single-stranded tails of the P4-P6 domain. Researchers have proposed that these tails participate in stabilizing triple-strand interactions with the P4 and P6 duplexes (12, 13). It therefore seemed likely that their removal would be destabilizing rather than providing the structural stabilization observed in P4-P6 fusion. Nevertheless, we tested the effect of these tails by constructing a new RNA that began with U107 and terminated with U258, using a cis-cleaving hammerhead ribozyme to generate the precise 5' terminus [C. A. Grosshans and T. R. Cech, *Nucleic Acids Res.* **19**, 3875 (1991)]. Fe(II)-EDTA cleavage analysis showed a pattern of protection similar to that of the original P4-P6 domain RNA, with a Mg²⁺ requirement that was at least as high (30). We conclude that the enhanced stability of the P4-P6 fusion RNA is not caused by removal of the 5' and 3' tails.
20. RNA samples (6 µg/ml) were incubated in 70 mM Mg²⁺ for 10 min at 50°C and then for 5 min at 42°C. RNA was then mixed with spermidine hydrochloride (250 µM final concentration), adsorbed to thin carbon supports, washed in 35 mM tris-HCl, pH 7.5, and 70 mM MgCl₂ for 1 min, passed through a graded ethanol series (50, 70, and 100% for 5 min each), air-dried, and rotary shadowcast with tungsten (21, 31). The experiment in the absence of Mg²⁺ was performed identically except that MgCl₂ was omitted from all solutions.
21. Y.-H. Wang, F. L. Murphy, T. R. Cech, J. D. Griffith, *J. Mol. Biol.* **236**, 64 (1994).
22. H.-M. Wu and D. M. Crothers, *Nature* **308**, 509 (1984); A. Bhattacharyya, A. I. H. Murchie, D. M. Lilley, *ibid.* **343**, 484 (1990); R. S. Tang and D. E. Draper, *Biochemistry* **29**, 5232 (1990); P. J. Hagerman, *Annu. Rev. Biochem.* **59**, 755 (1990).
23. F. L. Murphy, thesis, University of Colorado (1992).
24. The higher mobility of the folded domain is only observed in the presence of MgCl₂ (13 mM was provided in the gel and running buffer). In 100 mM NaCl, the native domain and various mutants with disrupted tertiary structure all comigrated (23). Thus, the Mg²⁺ requirement for tertiary folding is properly reflected in the electrophoretic assay.
25. P. A. Feldstein and G. Breuning, *Nucleic Acids Res.* **21**, 1991 (1993).
26. T. R. Cech, *Gene* **73**, 259 (1988).
27. J.-F. Wang, W. D. Downs, T. R. Cech, *Science* **260**, 504 (1993).
28. R. Green and J. W. Szostak, *J. Mol. Biol.* **235**, 140 (1994).
29. M. Chastain and I. Tinoco Jr., *Biochemistry* **31**, 12733 (1992); *ibid.* **32**, 14220 (1993). These authors reported that their model P4 and P6 helices were coaxially stacked, but the rotation between the two helices was approximately twice the normal rotation between consecutive base pairs. Their finding can be reconciled with our results in either of two ways. Either the displacement seen by Chastain and Tinoco is specific to their model P4-P6 RNA structure and not characteristic of the native P4-P6 domain, which is more highly constrained by tertiary interactions, or the displacement also occurs in the native P4-P6 domain but substituting a phosphodiester linkage does not perturb the structure significantly.
30. F. L. Murphy and T. R. Cech, unpublished data.
31. J. D. Griffith and G. Christiansen, *Annu. Rev. Biochem. Bioeng.* **7**, 19 (1978).
32. The plasmid encoding the P4-P6 fusion RNA was constructed from pP4P6 (9) with phagemid mutagenesis [T. A. Kunkel, J. D. Roberts, R. A. Zakour, *Methods Enzymol.* **154**, 367 (1987)]. We used two DNA oligonucleotides, one to delete nucleotides 105 and 106 and to insert nucleotides 240 through 258 between nucleotides 104 and 107, and a second one to delete nucleotides 235 through 261. Mutations were confirmed by dideoxynucleotide sequencing [F. Sanger, S. Nicklen, A. R. Coulson, *Proc. Natl. Acad. Sci. U.S.A.* **74**, 5463 (1977)]. The resulting plasmid was cleaved with Ear I endonuclease, such that transcription terminated with nucleotide 234.
33. J. M. Burke *et al.*, *Nucleic Acids Res.* **15**, 7217 (1987).
34. T. R. Cech, S. Damberger, R. R. Gutell, *Nat. Struct. Biol.* **1**, 273 (1994).
35. RNA was synthesized by transcription of plasmid DNA (32) in vitro with phage T7 RNA polymerase, purified by electrophoresis through a 7 M urea, 5% polyacrylamide gel, and 5'-end labeled with γ -³²P-labeled adenosine triphosphate (ATP) and polynucleotide kinase [J. A. Latham, A. J. Zaugg, T. R. Cech, *Methods Enzymol.* **181**, 558 (1990)]. We then allowed the RNA to refold by incubation for 10 min at 50°C in the indicated concentrations of MgCl₂ (Fig. 2). After 5 min at 42°C, Fe(II)-EDTA and dithiothreitol (DTT) were added; the final solution contained 35 mM tris-HCl (pH 7.5), 1 mM (NH₄)₂Fe(SO₄)₂, 2 mM Na₂-EDTA, 5 mM DTT, and 2, 13, or 50 mM MgCl₂. Because EDTA was in 1 mM excess over Fe²⁺, approximately 1 mM Mg²⁺ should have been chelated by EDTA; the free Mg²⁺ concentrations given in Fig. 2 were adjusted accordingly. After 80 min at 42°C, the reaction was stopped by addition of 10 mM thiourea and analyzed on a 7 M urea, 8% polyacrylamide gel.
36. H. Donis-Keller, A. M. Maxam, W. Gilbert, *Nucleic Acids Res.* **4**, 2527 (1977).
37. Gels contained 10% polyacrylamide with a 19:1 ratio of acrylamide:*N,N'*-methylenebisacrylamide. Both gel and electrophoresis buffer contained 13 mM MgCl₂ [A. M. Pyle, J. A. McSwiggen, T. R. Cech, *Proc. Natl. Acad. Sci. U.S.A.* **87**, 8187 (1990)].
38. We thank R. Gutell for help with Fig. 1 and A. Sirmarco for preparation of the manuscript. Supported in part by grants from the NIH (GM31819) and the American Cancer Society (NP583) (to J.D.G.) and by the W. M. Keck Foundation. T.R.C. is an Investigator of the Howard Hughes Medical Institute and an American Cancer Society Professor.

13 May 1994; accepted 29 July 1994